Feature Extraction and Pattern Recognition from Fisheye Images in the Spatial Domain

Konstantinos K. Delibasis[1] and Ilias Maglogiannis[2]
[1]*Dept. of Computer Science and Biomedical Informatics, Univ. of Thessaly, Lamia, Greece*
[2]*Dept. of Digital Systems, Univ. of Pireus, Greece*

Keywords: Omni-directional, Fisheye Image, Feature Extraction, Spatial Domain.

Abstract: Feature extraction for pattern recognition is a very common task in image analysis and computer vision. Most of the work has been reported for images / image sequences acquired by perspective cameras. This paper discusses the algorithms for feature extraction and pattern recognition in images acquired by omni-directional (fisheye) cameras. Work has been reported using operators in the frequency domain, which in the case of fisheye/omnidirectional images involves spherical harmonics. In this paper we review the recent literature, including relevant results from our team and state the position that features can be extracted from spherical images, by modifying the existing operators in the spatial domain, without the need to correct the image for distortions.

1 INTRODUCTION

The use of very wide field cameras is becoming very wide in domains like security, robotics, involving application such as silhouette segmentation, pose and activity recognition, visual odometry, SLAM and many more. Several types of cameras exist that offer 180^o field of view (FoV). These cameras are often called spherical, fisheye, or also omni-directional. The last term is also used for cameras with FoV close to 360^0, which may cause some confusion. We will use the terms interchangeably for the rest of the paper. A FoV of 180^0 or more, can be achieved using dioptric systems (spherical lens), or a combination of catadioptric (mirror, parabolic or spherical) and dioptric (lens). The 360^0 deg FoV omnidirectional cameras usually involve two mirrors and at least one lens. Both types of images can be treated in the same mathematic way, since in both cases the resulting images are defined over spherical coordinates (θ,φ) .

The use of this type of cameras is increasing in robotic and in video surveillance applications, due to the fact that they allow constant monitoring of all directions with a single camera. The price to pay is the very strong deformation induced by the camera, which involves rapid deterioration of spatial resolution towards the periphery of the FoV. This deformation has been studied by researchers, using a number of different image formation models. In principle, straight lines are imaged as conic curves. Thus, the images acquired by the fisheye camera are very different than the images acquired by perspective (projective) cameras. This induces extra complexity for image processing, as well as computer vision tasks.

In this work, we review some of the prominent work on image processing, feature extraction and pattern recognition from fisheye images and describe our results on a number of relevant tasks, using image processing techniques in the spatial domain, exploiting the calibration of the camera.

More specifically, results are presented for: a) redefining the Gaussian kernel in the spatial domain, without distortion correction, b) redefining Zernike moment invariants for calibrated fisheye images and applying them for human pose recognition, c) employing the camera calibration for human silhouette refinement, labelling and tracking and finally, d) using the main principles of image formation to detect human fall events using a single fisheye camera, without requiring exact calibration.

These results enhance our position that *efficient image processing and computer vision techniques can be achieved in the case of 180 deg FoV images, directly on the spatial image domain, without the need to employ spherical Fourier Transform, or perform distortion correction, or remap the image to different grid*.

Delibasis, K. and Maglogiannis, I.
Feature Extraction and Pattern Recognition from Fisheye Images in the Spatial Domain.
DOI: 10.5220/0006658704600465
In *Proceedings of the 13th International Joint Conference on Computer Vision, Imaging and Computer Graphics Theory and Applications (VISIGRAPP 2018) - Volume 4: VISAPP*, pages 460-465
ISBN: 978-989-758-290-5

2 METHODOLOGY

2.1 Fisheye Camera Calibration

Almost all the methods dealing with spherical images, assume a correspondence between image pixels and direction of view in the real world, preferably using the spherical coordinates (azimuth θ and elevation φ). This task is achieved by camera calibration. Image formation for fisheye is quite different than the simple projective (pinhole) camera. Several models for fisheye image formation have been proposed. In (Li H. and Hartley) and (Shah and Aggarwal 1996) the calibration of fisheye camera is reported using high degree polynomials to emulate the strong deformation introduced by the fisheye lens, radial and/or tangential. We have proposed a fisheye camera calibration (Delibasis, Plagianakos, and Maglogiannis 2014) that exploits the spherical reflection – central projection model, proposed by (Geyer and Daniilidis, 2001).

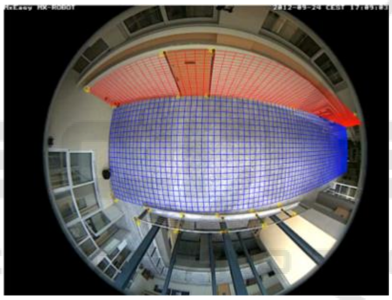

Figure 1: The achieved fisheye calibration, by reprojecting the floor and a wall, from (Delibasis, Plagianakos, and Maglogiannis 2014).

Further, we describe the inverse fish-eye camera model, i.e. obtaining the direction of view for any pixel (j,i) in the video frame, by defining two angles: the azimuth θ and the elevation φ. These angles are precalculated for every pixel of the frame and stored in a look-up table to accelerate dependent image processing tasks (Fig. 2).

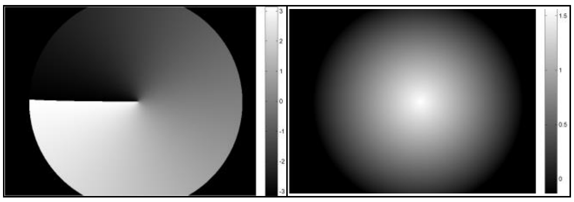

Figure 2: The azimuth and elevation for a fisheye image, from (Delibasis, Plagianakos, and Maglogiannis 2014).

2.2 Feature Extraction from Spherical Images

In (Hansen, Corke, Boles, Wageeh and Daniilidis, 2007), the well-known Scale-Invariant Feature Transform SIFT image descriptors that were introduced in (Lowe) are redefined for omnidirectional images. The implementation is performed in the frequency domain. However, since the image formation model uses spherical optical element and central projection, the omnidirectional image is defined over the space of spherical coordinates (azimuth θ and elevation φ). Thus, the image can be decomposed as a weighted sum of spherical harmonic functions $Y_l^m(\theta,\varphi)$ of degree l and order m, with $|m| \le l$. This decomposition is often called Spherical Fourier Transform (SFT). The Gaussian kernel has been defined in the (θ,φ) image domain using spherical harmonics of the 0th order (T. Bulow 2004)

$$G(\theta,\varphi;t)=\sum_l \sqrt{\frac{2l+1}{4\pi}}\,Y_l^0(\theta,\varphi)\,e^{-l(l+1)kt} \quad (1)$$

The Gaussian kernel may be projected on the omni-directional image, as shown in Fig. 1 of (Hansen, Corke, Boles, Wageeh and Daniilidis, 2007). However, in that work, the convolution of an image defined in the (θ,φ) space is defined in the frequency domain, using the SFT, rather than in the (θ,φ) space.

The work of (Cruz-Mota et al 2012) also employs the use of SFT to detect points of interest using the well-known SIFT. It is very interesting that the authors state "*we need to pass through the spherical*

Fourier domain because convolution on the sphere in spatial domain (3D) is hard (almost impossible) to compute"

Others have reported exploiting the image space, rather than the frequency domain, for specific kernels. In (Andreasson, Treptow, and Duckett, (2005)), the authors also used a simplified version of SIFT feature extraction method (eg. no multiresolution was used) for robot navigation by fisheye camera, obtaining good results, however there is no mention if the approach is optimal with respect to (Cruz-Mota et al 2012). In (Zhao, Feng, Wan, and Zhang, (2015)), features are extracted from 360 FoV omnidirectional images in the spatial domain, but after the image has been mapped to a hexagonal grid. In (Hara, Inoue, and Urahama, (2015)), 4-neighbours and 8-neighbours Laplacian operators have been proposed for omnidirectional panoramic images.

2.2.1 Geodesic Distance Metric between Pixels of the Calibrated Fish-eye Image

The formation of 180 FoV omni-directional image using a spherical lens can be summarized as following: the intersection of the line connecting the real world point with the center of the optical element is calculated with the optical element. This intersection is then projected centrally on the image sensor plane. It has been shown (Geyer and Daniilidis (2001)) that by choosing the center of projection, one can simulate the use of any quadratic shape mirror (spherical, ellipsoid, paraboloid and hyperboloid). This type of image formation induces non-linear transformation of distances between pixels.

In (Delibasis et al. 2016) we proposed the definition of geodesic distance between pixels, to replace the Euclidean distance, normally used for projective cameras. More specifically, since the geodesic curve of a sphere is a great circle, the distance between any two points on a sphere is the length of the arc, defined by the two points and belonging to the great circle that passes through the two points. The great circle has the same centre and radius with the sphere. Let $\mathbf{v}_0$ and $\mathbf{v}_1$ be the position vectors pointing to the unit sphere points P_0 and P_1. These points correspond to two pixels of the fisheye image. The distance of these two pixels is defined as the distance d of points P_0 and P_1 on the unit sphere and can be easily calculated as the arc-length between P_0 and P_1:

$$\mathbf{v}_0 \cdot \mathbf{v}_1 = \left(\cos\theta_0\cos\varphi_0, \sin\theta_0\cos\varphi_0, \sin\varphi_0\right) \cdot \left(\cos\theta_1\cos\varphi_1, \sin\theta_1\cos\varphi_1, \sin\varphi_1\right) \tag{2}$$

$$d = \cos^{-1}\left(\mathbf{v}_0 \cdot \mathbf{v}_1\right) \tag{3}$$

2.2.2 Definition of the Gaussian Kernel for Calibrated Fisheye Images

This distance metric can be applied to redefine the Gaussian kernel, by replacing the Euclidean distance in the exponent. Thus, a gaussian centered at pixel $\mathbf{p}_0 = \left(x_0, y_0\right)$ can be written as

$$g\left(x, y; \sigma\right) = g\left(\mathbf{p}; \sigma\right) = \frac{1}{2\pi\sigma_g^2} e^{-\frac{d(\mathbf{p},\mathbf{p}_0)^2}{2\sigma_g^2}} \tag{4}$$

These concepts are visualized in Figure 3, where the semi-spherical optical element of unit radius and the image plane is displayed. The center of projection is placed at $-f$ on the Y axis, with f set to 0.2 (a value obtained by the calibration of the actual Q24 Mobotix camera used in this work). The image plane is tessellated into 128 equidistant points to resemble the image pixels. 13 of these "pixels" (red dots in Fig.3a) are backprojected on the spherical optical element (both shown in different color). It is self-evident that the back-projected points are no longer equidistant.

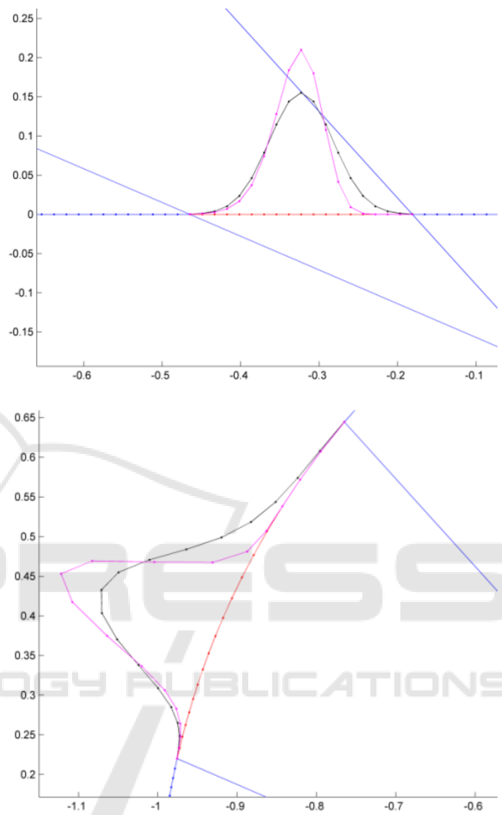

Figure 3: The Gaussian kernels generated using traditional/ planar and geodesic pixel distance (black and red curves respectively). The curves are placed (a) on the spherical lens and (b) on the image plane.

The definition of a Gaussian within the 13-pixel window, using the Euclidean distance between pixels on the image plane is visualized as the black curve in Fig. 3(a). If this Gaussian is back-projected on the spherical optical element, the kernel depicted in black at the periphery) is produced Fig. 3(a). As expected, it is substantially different from a Gaussian kernel, due to distance metric. In order to generate a Gaussian kernel defined on the image sensor, which is symmetric when applied on the spherical lens, we have to modify the distance metric between pixels on the sensor, according to the geodesic distance of their back-projection on the spherical lens.

2D Gaussian kernels, produced as above are shown in Fig. (4), at the center, and towards the periphery of the fisheye image.

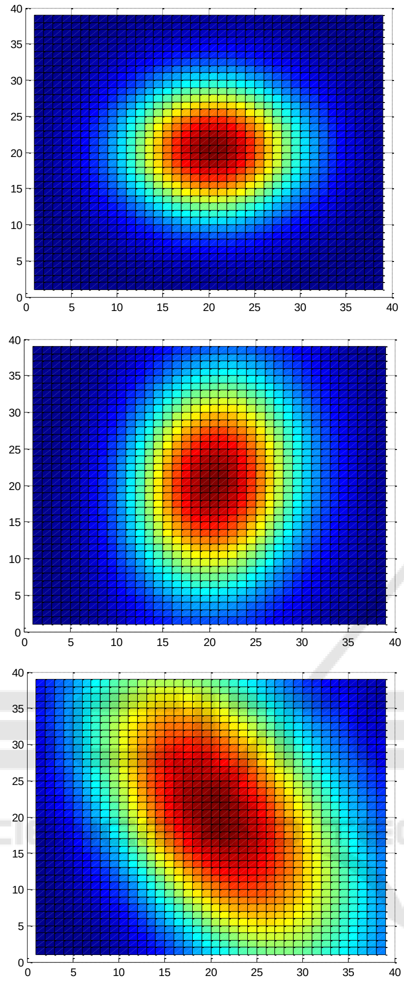

Figure 4: 2D Gaussian kernels, produced at the center (top) and towards the periphery of the fisheye image (bottom).

2.2.3 Definition of Zernike Moments in Calibrated Fish-Eye Image

Zernike moment invariants (ZMI) have been used regularly for pattern recognition in images and video sequences. The calculation of Zernike moments requires the distance and orientation with respect to the centre of the image patch, for each pixel of the segmented object / pattern to be classified. If the geodesic distance between pixels is used, then the ZMI can be calculated for the specific (calibrated) fisheye image.

$$Z_{nm} = \frac{n+1}{\pi} \sum_x \sum_y f(r,\theta) V_{nm}(r,\theta) \qquad (6)$$

where $V_{nm}(r,\theta) = R_{nm}(r) e^{jm\theta}$, r, θ are functions of (x,y).

$$R_{nm}(r) = \sum_{s=0}^{(n-|m|)/2} (-1)^s \frac{(n-s)!}{s!\left(\frac{n+|m|}{2}-s\right)!\left(\frac{n+|m|}{2}+s\right)!} r^{n-2s} \quad ..(7)$$

The substantial difference between traditional and geodesically corrected ZMI for a calibrated fisheye image is shown in Figure 5. The position of the application of the ZMI is indicated in Figure 5(a) by a yellow square.

(a) Fisheye image

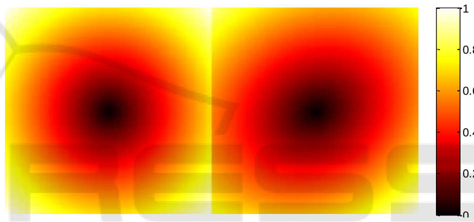

(b) Traditional (left) and corrected (right) pixel distance metric

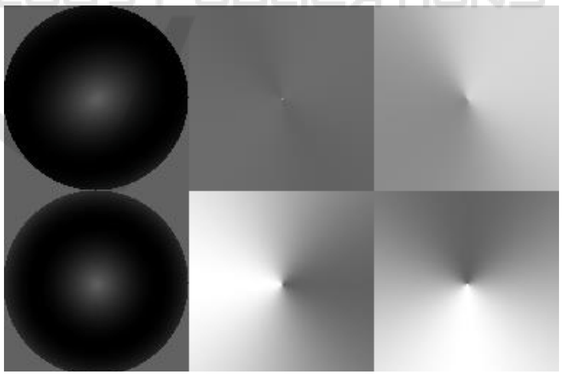

(c) The resulting Zernike radial polynomial and angular terms

Figure 5: Differences in the planar (left) and geodetic definition (right) of (b) distance and (c) angle between two image pixels, from (Delibasis et al. 2016).

2.2.4 Silhouette Segmentation in Calibrated Fish-Eye Image

In (Delibasis et al. 2014) a refinement for the segmentation of human silhouettes was proposed, using spatial relations of the binary objects/parts of a segmented silhouette, using clues from the calibration of the fisheye camera. Results showed that the method was quite robust, as well as computationally efficient. Figure 6 shows a composite frame with segmented silhouettes (a), as well as the estimated trajectory in real world coordinates (b).

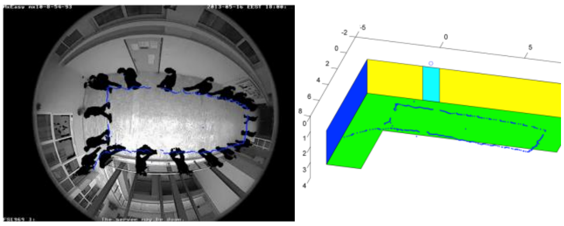

(a) (b)

Figure 6: Silhouette segmentation and tracking through a fisheye camera, from (Delibasis et al. 2014).

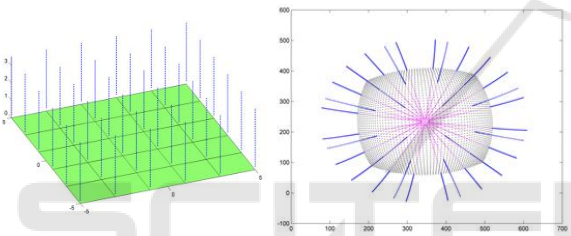

Figure 7: Real world vertical lines and their rendering through a fisheye camera with vertical optical axis, from (Delibasis et al. 2015).

2.2.5 Fall Detection by Uncalibrated Fish-eye Camera

In (Delibasis, and Maglogiannis, (2015)) a simple and effective algorithm was proposed to detect falling events of humans monitored by fisheye camera. Instead of the full calibration of the camera, the only requirement was that the camera axis should point parallel to the vertical axis. The proposed algorithm exploits the model of image formation to derive the orientation in the image of elongated vertical structures. World lines are imaged as parts of curves, which, if extrapolated (equivalently extending the 3D vertical lines to infinity), will all intersect at the center of the camera's field of view (FoV). Lines parallel to the optical axis are rendered as straight lines. Line extrapolation is shown in dotted style (Figure 7). The floor is drawn as it would appear at z=3.5 meters from the ceiling where the camera is installed.

The proposed fall detection algorithm consists of the following simple steps:

1. The center of the FoV is detected (offline, for a single video frame).
2. For each video frame:
   - 2.1. The silhouette is segmented
   - 2.2. Its major axis is calculated
   - 2.3. If the silhouette is sufficiently elongated and its major axis does not point close to the center of FoV, then the silhouette is assumed to correspond to a falling person

3 RESULTS

The proposed geometry-based silhouette refinement algorithm was applied to 5 video sequences. Two classes of pixels were considered: pixels that belong to human silhouettes inside the room (excluding any other activity) and the rest of the pixels. Table 1 shows the confusion matrix for the segmentation of the, with and without the application of the proposed algorithm – (1st row true positive -TP, false negative pixels -FN, 2nd row: false positive -FP, true negative pixels -TN). It can be observed that the number of TP and FN pixels remain almost the same with and without the application of the geometry-based refinement. The number of FP pixels decreases significantly, whereas TN increases with the application of the proposed algorithm.

Table 1: The confusion matrix of the human silhouette segmentation for 5 videos, with and without the application of the proposed geometry-based algorithm from (Delibasis et al. 2014).

Segmentation only		Segmentation and geometry-based silhouette refinement	
172388	21828	172109	22085
142676	48815108	23725	48934081

In (Delibasis, et al. 2016), the *Zernike Moment Invariants (ZMI) for the calibrated fisheye* image were tested against the traditional ZMI in a problem of pose recognition. Synthetic video frames were used for training and testing. Testing was performed on real video frames, as well. The achieved results for synthetic data (5 different poses) are shown in Table 2. The superiority of the proposed ZMI, is evident, although marginal. More experimentation can be found in (Delibasis, et al. 2016), which validates these findings.

Table 2: The classification accuracy of the segmented silhouette pose for different orders of the traditional radial Zernike implementation (Delibasis, et al. 2016).

Zernike Degree *n*, Order *m*	Geodesic correction	Classification Accuracy (%)	
		Video 1	Video 2
n = 2,4,6,8,10, *m*=0	NO	93.39	94.53
	YES	94.09	96.13
n = 2,4,6,8,…,20, *m*=0	NO	91.68	94.14
	YES	94.24	95.94
n = 2,4,6,8,…,30, *m*=0	NO	92.11	94.01
	YES	92.24	95.75

The proposed algorithm for *fall detection* has been applied to two video sequences containing 5 fall events, acquired by the fish-eye camera at 15 fps frame rate of 480x640 pixels. The confusion matrix for both videos is shown in Table 3.

Table 3: Confusion matrix for fall classification, from (Delibasis and Maglogiannis, 2015).

	Standing	Not Standing	Undefined
Standing	1374	256	388
Not Standing	513	1684	

4 CONCLUSIONS

A number of image processing and computer vision tasks have been presented, applied to images and videos acquired by a calibrated fisheye camera. First we defined a metric for pixel distances, based on the image formation model. Subsequently we applied this metric to the definition of the Gaussian kernel, as well as to the re-definition of Zernike Moment Invariants (ZMI). The corrected ZMI outperformed the traditional ones for pose recognition. Two more applications, involving silhouette segmentation and fall detection, the later one without the requirement for full fisheye calibration were reviewed. All these fisheye-specific processing tasks were applied to spatial domain, without the need to remap the image to different grids, or correct for the strong distortions. These results support our position, that efficient image processing and analysis algorithms can be performed directly in the fish-eye image domain. Further work includes the application of a number of other feature extraction algorithms, such as SIFT, Harris corner detection and Hough Transform.

REFERENCES

Hansen, P., Corke P., Boles W. and Daniilidis, K. (2007) Scale Invariant Feature Matching with Wide Angle Images. In *Proceedings IEEE/RSJ International Conference on Intelligent Robots and Systems, pages pp. 1689-1694, San Diego, USA.*

Lowe D., “Distinctive image features from scale-invariant keypoints,” *International Journal of Computer Vision, vol. 60, no. 2*, pp. 91–110, 2004.

Bulow,T., “Spherical diffusion for 3D surface smoothing,” *IEEE Transactions on Pattern Analysis and Machine Intelligence, vol. 26, no. 12*, pp. 1650–1654, Dec 2004.

Hara, K., Inoue, K., and Urahama, K. (2015). Gradient operators for feature extraction from omnidirectional panoramic images. *Pattern Recognition Letters, 54, 89-96.*

Cruz-Mota, J., Bogdanova, I., Paquier, B., Bierlaire, M., and Thiran, J. P. (2012). Scale invariant feature transform on the sphere: *Theory and applications. International journal of computer vision, 98(2), 217-241.*

Andreasson, H., Treptow, A., and Duckett, T. (2005). Localization for mobile robots using panoramic vision, local features and particle filter. In *Robotics and Automation, 2005. ICRA 2005. Proc. of the 2005 IEEE International Conference on* (pp. 3348-3353).

Zhao, Q., Feng, W., Wan, L., and Zhang, J. (2015). SPHORB: a fast and robust binary feature on the sphere. *International Journal of Computer Vision, 113(2)*, 143-159.

Li H. and Hartley R., Plane-Based Calibration and Auto-calibration of a Fish-Eye Camera, in P.J. Narayanan et al. (Eds.): ACCV 2006, LNCS 3851, pp. 21–30, 2006, *Springer-Verlag Berlin Heidelberg 2006.*

Shah S. and Aggarwal J. 1996, Intrinsic parameter calibre-tion procedure for a high distortion fish-eye lens camera with distortion model and accuracy estimation, *Pattern Recognition*, 29(11), 1775- 1788, 1996.

Delibasis, K. K., Plagianakos, V. P. and Maglogiannis, I. “Refinement of human silhouette segmentation in omni-directional indoor videos,” *Computer Vision and Image Understanding, vol. 128, pp. 65-83, 2014.*

Delibasis, K. K., S. V. Georgakopoulos, K. Kottari, V. P. Plagianakos, and I. Maglogiannis. (2016) "Geodesically-corrected Zernike descriptors for pose recognition in omni-directional images." *Integrated Computer-Aided Engineering, Preprint (2016): 1-15.*

Geyer, C., and Daniilidis, K. (2001). Catadioptric projective geometry. *International journal of computer vision, 45(3), 223-243.*

Delibasis, K. K., and Maglogiannis, I. (2015). A fall detection algorithm for indoor video sequences captured by fish-eye camera. In *Bioinformatics and Bioengineering (BIBE), 2015 IEEE 15th International Conference on (pp. 1-5).*